

Tissue-engineered cartilage constructed by a biotin-conjugated anti-CD44 avidin binding technique for the repairing of cartilage defects in the weight-bearing area of knee joints in pigs



**H. Lin,
J. Zhou,
L. Cao,
H. R. Wang,
J. Dong,
Z. R. Chen**

Zhongshan Hospital,
Fudan University,
Shanghai, China

Objectives

The lack of effective treatment for cartilage defects has prompted investigations using tissue engineering techniques for their regeneration and repair. The success of tissue-engineered repair of cartilage may depend on the rapid and efficient adhesion of transplanted cells to a scaffold. Our aim in this study was to repair full-thickness defects in articular cartilage in the weight-bearing area of a porcine model, and to investigate whether the CD44 monoclonal antibody biotin-avidin (CBA) binding technique could provide satisfactory tissue-engineered cartilage.

Methods

Cartilage defects were created in the load-bearing region of the lateral femoral condyle of mini-type pigs. The defects were repaired with traditional tissue-engineered cartilage, tissue-engineered cartilage constructed with the biotin-avidin (BA) technique, tissue-engineered cartilage constructed with the CBA technique and with autologous cartilage. The biomechanical properties, Western blot assay, histological findings and immunohistochemical staining were explored.

Results

The CBA group showed similar results to the autologous group in biomechanical properties, Moran's criteria, histological tests and Wakitani histological scoring.

Conclusions

These results suggest that tissue-engineered cartilage constructed using the CBA technique could be used effectively to repair cartilage defects in the weight-bearing area of joints.

Cite this article: *Bone Joint Res* 2017;6:284–295

Keywords: Biotin, Avidin, Cartilage defects

- H. Lin, MD, PhD, Associate Professor,
- J. Zhou, MD, PhD, Attending Surgeon,
- L. Cao, MD, PhD, Resident Surgeon,
- H.R. Wang, MD, PhD, Resident Surgeon,
- J. Dong, MD, PhD, Professor,
- Z.R. Chen, MD, PhD, Professor, Department of Orthopedic Surgery, Zhongshan Hospital, Fudan University, 180 Fenglin Road, Shanghai 200032, China.

Correspondence should be sent to Z.R. Chen;
email:
chenzhengrong99@126.com

doi: 10.1302/2046-3758.65.BJR-2016-0277

Bone Joint Res 2017;6:284–295.
Received: 15 October 2016;
Accepted: 20 February 2017

Article focus

- To investigate whether the CD44 monoclonal antibody biotin-avidin (CBA) binding technique could provide better tissue-engineered cartilage
- To investigate whether the tissue-engineered cartilage constructed with CBA binding technique could effectively repair cartilage defects in the weight-bearing area of knee

Key messages

- The regeneration of a specific hyaline cartilage to repair the cartilage defects in

weight-bearing area could be achieved using tissue engineered cartilage constructed with CBA technique.

- There is considerable potential for the tissue-engineered cartilage constructed by CBA technique to clinically repair the cartilage defects in the weight-bearing area.

Strengths and limitations

- Compared to cartilage from non-weight-bearing area, the restoration of defects within the weight-bearing area in our study is more important for clinical practice.

- In our study, the porcine joint size and gait characteristics more accurately represent humans compared with smaller animals, so it is more appropriate for translation of cartilage treatment strategies toward use with humans.
- More preclinical studies should be explored before the tissue-engineered cartilage constructed by CBA technique is used clinically for the repair of cartilage defects.

Articular cartilage is prone to damage and degenerative change. Avascular and articular chondrocytes are highly differentiated and have limited self-repairing capacity. Damage to articular cartilage provokes a limited healing response and frequently progresses to osteoarthritis (OA). Everybody aged > 65 years has some clinical or radiographic evidence of OA.² The goal in the treatment of injury to articular cartilage and OA is improved repair and the restoration of mechanically functional cartilage tissue.³

Various ways of repairing articular cartilage have been tried including arthroscopy and debridement, subchondral drilling, microfracture, auto-cartilage (or auto-chondrocyte) transplant, allograft cartilage (or allograft chondrocyte) transplant and periosteal or perichondrial transplant.⁴⁻⁷ Each has had some success and may temporarily alleviate symptoms. However, a fibrocartilage repair tissue is produced, which is biomechanically inferior to hyaline cartilage, and these methods may themselves result in degenerative changes in the long term.⁸⁻¹⁰ Attention has turned to tissue engineering techniques for the next generation of cartilage regeneration and repair solutions. This involves combining a variety of cell sources, scaffold materials and bioactive factors to induce the formation of active living tissue *in vivo*.¹¹⁻¹² It has been shown to be a promising approach for restoring the morphology, structure and function of damaged articular cartilage.¹³ The overriding principle of tissue-engineered repair of cartilage is that the seeding chondrocytes synthesise and deposit the components of extracellular matrix (ECM) and integrate repair tissue with the surrounding host tissue. Success may depend on the initial adhesion of chondrocytes to a scaffold.¹⁴ Tissue-engineering scaffolds play a role similar to that of ECM in natural tissues, supporting the adhesion and proliferation of cells. However, due to a lack of ECM adhesion proteins for specific interactions, the attachment of cells to artificial biomaterials is merely mediated by non-specific interactions such as ionic attraction, hydrogen bonding and hydrophobic interaction. Cells adhere rather poorly to synthetic biomaterials, and hamper effective repair of the cartilage. The adhesion of cells in three dimensional (3D) scaffolds is crucial if cell anoikis is to be avoided, and this is one of the most important issues in fundamental cell biology.^{15,16} In order to encourage the adhesion of cells, immobilisation of bioactive molecules such as arginine-glycine-aspartic acid

(RGD) peptide, hydroxyapatite or natural polysaccharide is a common strategy to ensure controlled interaction between the cells and the scaffold.¹⁷⁻¹⁹ These methods are based on the formation of integrin-mediated bonds between substrata and the cell membrane. Their efficacy will depend on the availability of cell membrane receptors. Cells possessing few functional integrins might not benefit from these methods.

This problem could be solved by using a binding mechanism separate from the integrin-binding system. The biotin-avidin based system is one of the most investigated binding protein-ligand couples and is used in many biotechnological applications. This technology is based on the extraordinary affinity of avidin for biotin ($KD = 10^{-5} M^{-1}$).^{20,21} The highly specific binding capability between these two molecules could mediate the attachment of cells onto biomaterial surfaces. When used in tissue engineering, it is known that almost all kinds of cells have abundant amine groups on their membranes, which can be biotinylated by N-hydroxysuccinimide-D-biotin (NHS-D-biotin). Biotinylated cells have been cultured on avidin-modified surfaces, and the enhanced adhesion of cells is achieved through specific biotin-avidin interaction.^{22,23} The mechanism by which the biotin-avidin system improves the adhesion of chondrocytes is illustrated in Figure 1a.

However, one problem hinders the use of the biotin-avidin approach. The binding efficacy of biotinylated cells to avidin-coated substrata decreases over time. This may be attributed to the endocytosis of cell membrane biotin molecules which decreases the strength of binding between the biotinylated cells and avidin-coated substrata, and therefore undermines the use of the biotin-avidin system in the long-term adhesion of cells and cell culture.²⁴

Since the molecular size of biotin is small, it is easy for biotin to attach to biomolecules, including antibodies, without interfering with molecular functions. CD44 is an isomeric family of surface molecules expressed on a wide variety of cell types, including chondrocytes.^{25,26} In our previous work, the biotin was conjugated to monoclonal anti-CD44 antibodies, and then formed bonds with avidin on scaffolds, as shown in Figure 1b. Our results showed that the ability of chondrocytes to adhere to scaffolds prepared by the CD44 monoclonal antibody biotin-avidin (CBA) binding technique led to improved cartilage tissue engineering.²⁷ However, *in vivo* repair of cartilage defects with the tissue-engineered cartilage constructed with the biotin-conjugated anti-CD44 antibody-avidin binding system, especially for defects in the weight-bearing area, remains to be explored. Thus, the current study was designed to repair full-thickness articular cartilage defects in the weight-bearing area in a porcine model, and to investigate whether the CBA binding technique could provide better tissue-engineered cartilage for clinical applications.

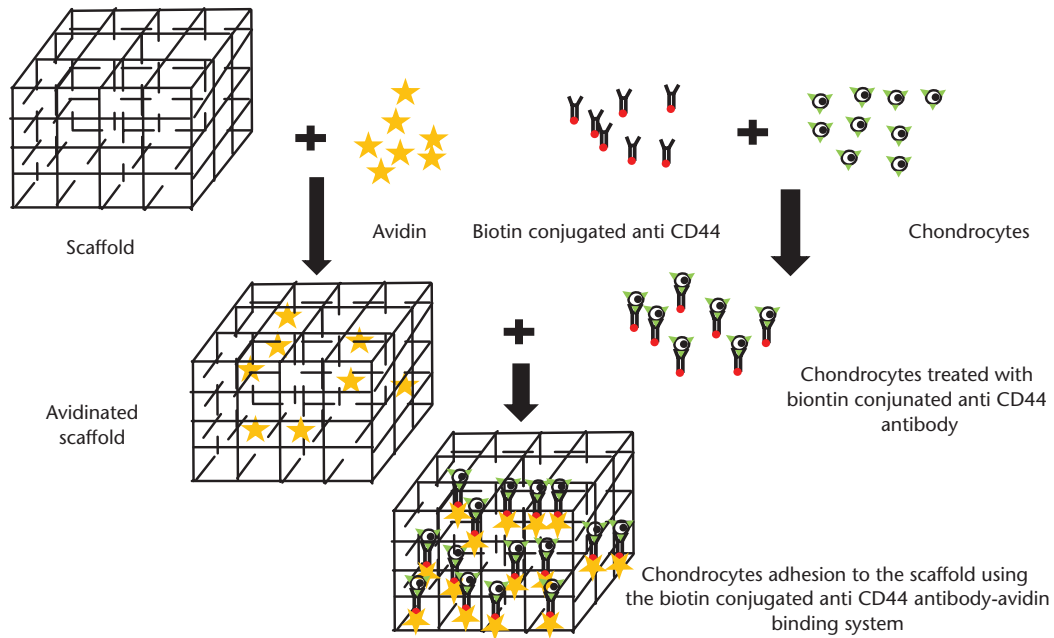


Fig.1a

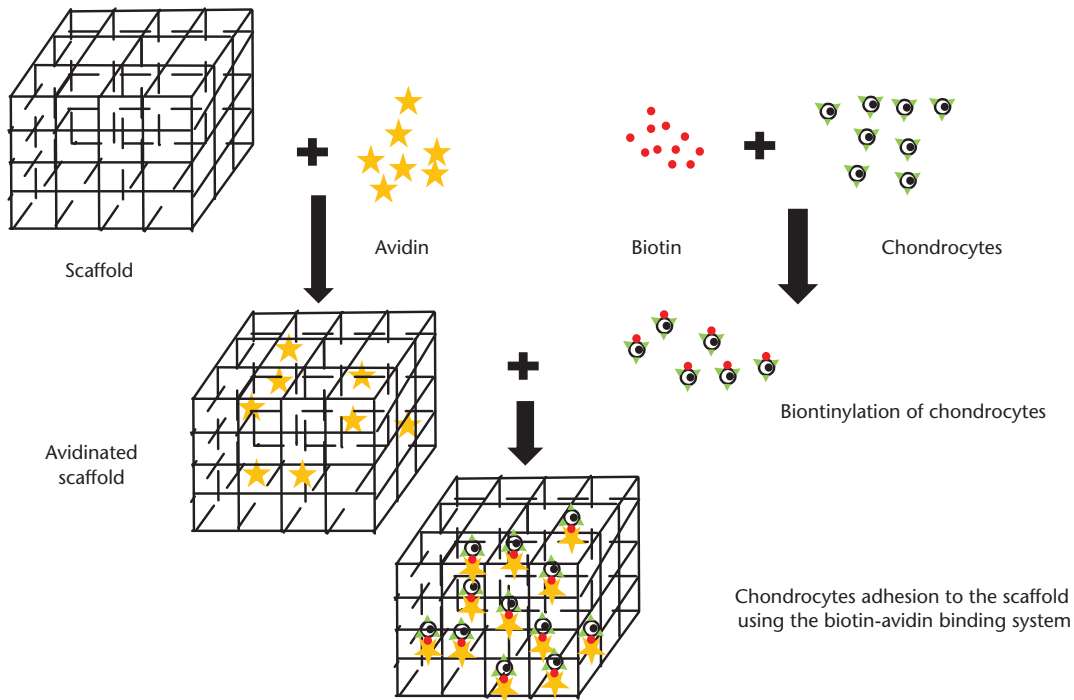


Fig.1b

a) the biotin–avidin system, the biotin was conjugated to cell membrane, and the avidin was immobilised to the scaffold. The bond formation between biotin and avidin mediated chondrocyte adhesion to the scaffold; b) The biotin-conjugated anti-CD44 antibody–avidin binding system, where the biotin avidin was used as a bridge connecting the scaffold and the antibodies, and the monoclonal anti-CD44 antibodies were used as the bridge connecting the chondrocytes and the biotin.

Materials and Methods

All animal procedures were performed at the animal centre of Zhongshan Hospital with ethical approval from the Animal Care and Use Committee of Fudan University (Shanghai, China).

Preparation of chondrocytes. Cartilage was collected aseptically from the knee and hip joints of five-week-old porcine (Animal Center, Zhongshan Hospital, Fudan University). First, it was rinsed with phosphate buffer solution (PBS), divided with a scalpel, and washed twice

with PBS. The ECM was digested in Dulbecco's Modified Eagle's Medium (DMEM; Biowest, Nuaille, France), containing 0.2% type II collagenase (Sigma-Aldrich, St Louis, Missouri), at 37°C in a water bath and shaken for two hours. The tissue debris was removed by filtration using a 40 µm sieve, and chondrocytes in the filtrate were collected by centrifugation at 300 g for ten minutes. They were re-suspended and cultured in complete DMEM with 10% foetal bovine serum (FBS; GE Healthcare, Logan, Utah), 100 U/mL penicillin, and 100 µg/mL streptomycin. The cell suspension was adjusted to a density of 2×10^5 /mL, seeded into 75 cm² flasks (Corning Inc, Corning, New York), and cultured at 37°C with 5% CO₂. The culture medium was changed every two to three days. Confluent chondrocytes were passaged at a ratio of 1:3, and passage 2 chondrocytes were used.

The construction of tissue-engineered cartilage with biotin-conjugated anti-CD44 avidin binding system. Porous chitosan scaffolds were prepared as follows: 10 mL chitosan solution was poured into a mould, frozen at -20°C for 24 hours, and immersed in -5°C ethanol for another 24 hours. After removing the mould, the well-shaped scaffold with ethanol was equilibrated at room temperature for two hours. The scaffold was then put into 5% NaHCO₃ solution to neutralise the residual acetic acid for six hours, and finally washed with de-ionised water five times. The scaffold was prepared with a diameter of 10 mm and a height of 3 mm. Its porosity was > 90%, and the pore diameter was 100 µm to 150 µm. It was sterilised with ethylene oxide.

Avidination of the porous chitosan scaffold. The avidination of the porous scaffolds was performed in accordance with the manufacturer's recommended procedure and with previous studies.²⁸ The prepared scaffold was placed in a 12-well plate to which 3.0 mL of 0.1 mg/mL avidin solution was added, and the plates were incubated in a shaker for one hour at room temperature. The scaffold was washed twice with PBS containing 100 U/mL penicillin, 100 µg/mL streptomycin and 25 mg/mL amphotericin B, and air-dried.

Tissue-engineered cartilage constructed with biotin-conjugated anti-CD44 avidin binding system. The tissue-engineered cartilage was divided into three groups: group 1, chitosan scaffold + chondrocytes (control group); group 2, avidinised porous chitosan scaffold + biotinylated chondrocytes (BA group); and group 3, avidinised porous chitosan scaffold + chondrocytes treated with biotin-conjugated anti-CD44 (CBA system group). The tissue-engineered cartilage was constructed as described previously²⁸. Briefly, 5×10^7 /mL of chondrocytes were treated with biotin (Sigma-Aldrich) for 30 minutes (1 mg biotin / 1×10^6 chondrocytes) or biotin-conjugated anti-CD44 antibody (BioLegend, San Diego, California) (0.25 µg of CD44 monoclonal antibody biotin / 1×10^6 chondrocytes), and washed twice with PBS. The chondrocytes were then seeded into the scaffolds in the 24-well

plate (200 µL cell suspension per scaffold). The chondrocyte-scaffold complexes were cultured in a CO₂ incubator, at 37°C with atmosphere containing 5% CO₂. Four hours after the initial seeding, the complexes were transferred to another 24-well plate. The culture medium was collected and the detached chondrocytes were counted in a blood counting chamber and the ratio of detachment was calculated. Fresh culture medium (2 mL) was added to the new 24-well plate with the chondrocyte-scaffold constructs. The 24-well plate was then placed in a CO₂ incubator and the culture medium was renewed every two days. Except for the complexes that were tested for real-time polymerase chain reaction, the remaining chondrocyte-scaffold complexes were transplanted to repair the full-thickness defects of the articular cartilage of the knees in the pigs.

Repair of the full-thickness defects of weight-bearing knee-joint articular cartilage in pigs. We obtained 28 mini-type pigs (three months old; mean weight, 15 kg, SD 2.5; gender not considered). They were checked to ensure that there were no visible wounds, infection or deformity near the knees. Anaesthesia was induced by muscular ketamine, 10 mg/kg. Using a sterile technique, a medial parapatellar incision was made in both hind limbs, followed by a lateral parapatellar arthrotomy. The patella was retracted medially, and full-thickness cartilage defects (10 mm diameter, 3 mm depth) were created by trepan on the load-bearing region of the lateral femoral condyle (Fig. 2). A total of 52 full-thickness defects were created. Two pigs died while under anaesthetic.

The experimental groups included: a full-thickness defect repaired with traditionally engineered cartilage (control group, n = 12); a full-thickness defect repaired with engineered cartilage constructed by biotin-avidin binding technique (BA group, n = 12); a full-thickness defect repaired with engineered cartilage constructed by CBA binding technique (CBA group, n = 12); a full-thickness defect repaired with the plug harvested when creating the defect (auto group, n = 12). The defects were randomly assigned into the four groups, with 12 defects in each group. Two pigs (four defects) were used as the blank control and received no treatment. The tissue-engineered articular cartilage (or autologous articular cartilage) was transplanted into the defects after the basal region was sprayed with medical adhesive. After thorough haemostasis, the incision was closed in layers using absorbable sutures. Each pig received 2.4×10^5 units of gentamicin intramuscularly during and after the surgery to prevent infection. Movement and weight-bearing were allowed as tolerated after surgery. At 12 and 24 weeks after surgery, respectively, 12 pigs in the experimental group (three in each group) and one in the blank group were killed with an overdose of pentobarbital. The hind limbs were disarticulated at the hip. Six samples from each group were used for the testing at each time.

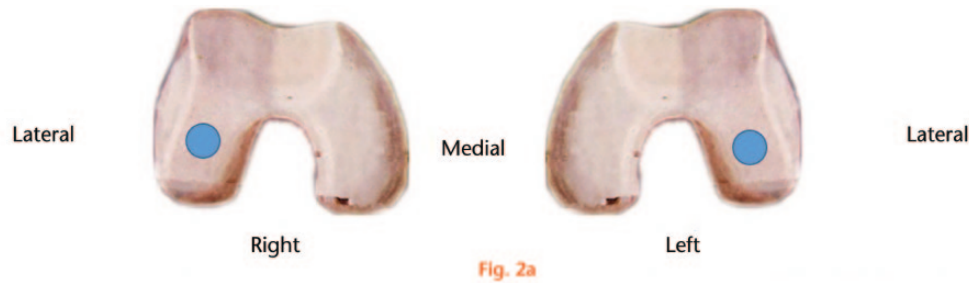


Fig. 2a

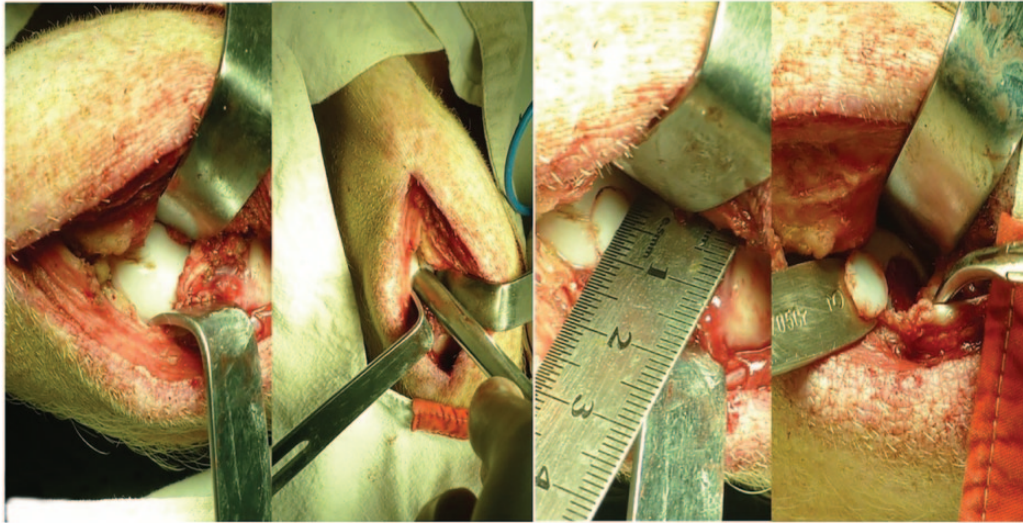


Fig. 2b

a) Schematic image showing the location of the cartilage defects on the load-bearing region of the lateral femoral condyle; b) the surgical approach showing location of cartilage defects on the lateral femoral condyle.

Evaluation and methods: cell detachment assay. Four hours after the initial seeding, the chondrocyte-scaffold complexes were transferred to another 24-well plate for further culture. The culture medium was collected and the detached chondrocytes were counted in a blood counting chamber, and the ratio of detachment was counted using a blood counting instrument (N_{un}). The ratio of detachment was calculated using formulae 1 and 2, below. A lower ratio meant a higher ratio of planted chondrocytes and a stronger adhering ability.

Formula (1):

$$\begin{aligned} &\text{Ratio of detachment of planted chondrocytes} \\ &= N_{un} / N_0 \times 100\% \end{aligned}$$

Formula (2):

$$N_0 = 5 \times 10^7 / \text{mL} \times 200\mu\text{L}$$

Evaluation and methods: Real-time PCR. The gene expressions of the constructs were examined during *in vitro* differentiation. One week after culture, the chondrocyte-scaffold complex was harvested for the extraction of RNA. TRIzol (Invitrogen, Carlsbad, California) was used to extract the total RNA according to the manufacturer's

protocol. After resuspending in 30 μL DNase/RNase-free water, the concentration and purity were checked by the ratio of the absorbance at 260 and 280 nm and measured using a spectrophotometer (FP-6500; JASCO Inc., Tokyo, Japan). Subsequently, 2 μg of RNA was reverse transcribed into cDNA using a reverse transcription system (Promega, Fitchburg, Wisconsin). Subsequently, the real-time PCR (RT-qPCR) was carried out on a Bio-Rad iCycler (Bio-Rad Laboratories, Hercules, California). The real-time PCR was initiated with a two-minute 50°C hold, followed by a ten-minute 95°C hold, and then continued with 40 cycles of 15 seconds at 95°C and one minute at 60°C.

Evaluation and methods: Gross view. The activity, feeding behaviour and wound healing of the pigs after surgery were recorded. After being killed by intravenous pentobarbital 12 or 24 weeks after surgery, the knee and implants were harvested. After an examination for findings suggestive of rejection or infection, such as severe inflammation or extensive fibrosis, the degree of cartilage repair was grossly evaluated. The colour, lustre, irregularity, presence of depression or bulging of the repaired tissue in the defect and the state of the border with the surrounding normal cartilage tissue, were

examined carefully. The midline of the defects was dissected in order to see the longitudinal cross-section, and the interface between the repaired tissue and adjacent normal osteochondral tissue. The regenerated cartilage was scored macroscopically according to Moran's criteria at each time point.²⁹ A higher grade represents a better repair. The scoring was performed as a blind test by three independent researchers (JZ, LC, HRW).

Evaluation and methods: biomechanics tests. The biomechanical properties of the samples used for these analyses were immediately evaluated under fresh conditions. They were trimmed along the rim of the regenerated tissue using a trephine. The corresponding normal articular cartilage samples were harvested by the same method. The biomechanical property of the engineered cartilage was tested by measuring the compressive modulus as described previously.^{10,30} Briefly, the harvested parts (5 mm in diameter) were fixed onto a sample table of the biomechanical analyser TMI UTM-10T (Toyo Baldwin Co., Tokyo, Japan). A force-displacement curve was obtained by applying a constant compressive strain at a rate of 0.5 mm/min until reaching the maximal force at 400 N. Each sample underwent five indentation tests. The elastic modulus and stiffness were calculated from the curve using formulae 3 and 4.

Formula (3):

$$E = (F/A_0) / (\Delta L/L_0)$$

Formula (4):

$S = F / \Delta L$ (E, elastic modulus (Mpa); F, acting force (N); S, stiffness (N/mm); A_0 , contact area before test (m^2); L_0 , height of the sample before the test (m); ΔL , height variation of the sample after the test (m)).

As the defects in the control group at 12 weeks were filled with a small amount of fibrous tissue, which further collapsed at 24 weeks, biomechanical tests on the regenerated tissue could not be performed properly.

After the biomechanical tests, one half of each sample was used for histological examination and immunohistochemical staining, while the glycosaminoglycan (GAG) content of the other half was determined.

Evaluation and methods: Western blot assay. After the biomechanical analysis, the samples were collected. Western blotting methods were used to detect the collagen II (COL II) and aggrecan proteins. The tissue was homogenised with Pierce T-PER tissue protein extraction reagent (Thermo Fisher Scientific Inc., Waltham, Massachusetts) according to the manufacturer's instructions. The total quantity of protein was determined using the Pierce BCA Protein Assay Kit (Thermo Fisher

Scientific Inc.). Samples were loaded onto 10% to 14% SDS-PAGE (Beyotime Biotechnology, Shanghai, China) gels and transferred to a polyvinylidene fluoride membrane (Merck Millipore, Billerica, Massachusetts). The membranes were then blocked with 5% skimmed milk in 0.05% tris-buffered saline/Tween 20 (TBST), followed by incubation with the indicated antibodies at their recommended dilutions in Western blocking buffer (WBB, PBS, 5% powdered milk, 0.1% Tw-20). Samples were then incubated with horseradish peroxidase (HRP)-conjugated secondary antibody, followed by enhanced chemiluminescence detection (ImageJ, National Institute of Health, Maryland). Chemiluminescence detection values were used to quantitate the Western blot results. A ratio of each band of interest to the internal control was obtained and the statistical significance of differences between control and experimental groups determined.

Evaluation and methods: histological analysis. Specimens were fixed with buffered formalin and decalcified in a solution of ethylenediamine tetra-acetic acid (EDTA) in a shaker. The samples were dehydrated with a gradient ethanol series, cleared with xylene, and embedded in paraffin blocks. Sections, 5 mm thick, were obtained and stained with haematoxylin and eosin (H&E) and toluidine blue (TB) for histological analysis.

According to the scoring system described previously by Wakitani et al,³¹ the histological structure, matrix staining, surface regularity and thickness of the repaired cartilage, and the integration of the repaired tissue with its surrounding normal tissue were graded blindly by three observers (JZ, LC, HRW).

Evaluation and methods: immunohistochemical staining. The expression of COL II in the engineered cartilage was examined by immunohistochemical staining at 12 and 24 weeks after implantation. Briefly, paraffin sections were deparaffinised followed by hydration in ethanol solutions of decreasing concentrations (100% to 70%), and pre-treated with 0.1% of Proteinase K (Vivantis Technologies, Oceanside, California) at room temperature for 30 minutes. The sections were then treated with protein blocking agent (UltraTech HRP Kit, Beckman Coulter France, Villepinte, France) for ten minutes and incubated with goat serum to block non-specific sites. The slides were washed in PBS three times and the sections were incubated at 37°C for one hour with mouse anti-collagen type II monoclonal antibody diluted in PBS (1:200), followed by incubation with 1:100 diluted horseradish peroxidase (HRP)-conjugated anti-mouse antibody (Dako, Carpinteria, California) for 30 minutes. Colour was developed with diaminobenzidine tetrahydrochloride (DAB).

Statistical analysis. Normality testing was carried out using SPSS 16.0 software (IBM Corp., Armonk, New York) and the values were expressed as mean SD ($\bar{x} \pm s$). One-way analysis of variance (ANOVA) was also carried out. Statistical significance was set at a p-value < 0.05.

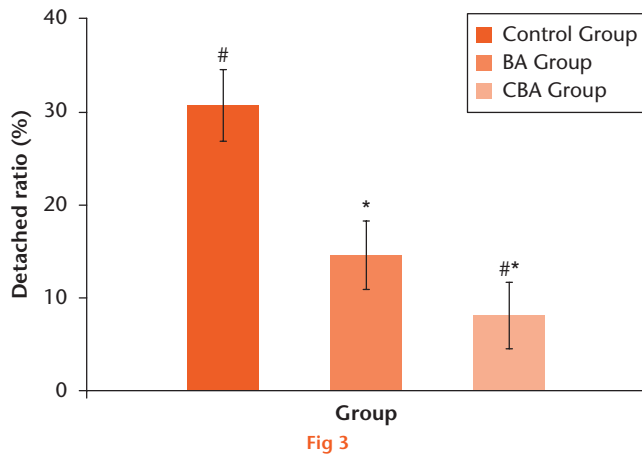


Fig 3

Chart showing the ratio of chondrocyte detachment in control, BA and CBA groups after the chondrocytes were planted in the scaffold for four hours. Analysis of variance and least-significant differences (LSD) test compared with control group, * $p=0.001$; compared with BA group, # $p=0.002$.

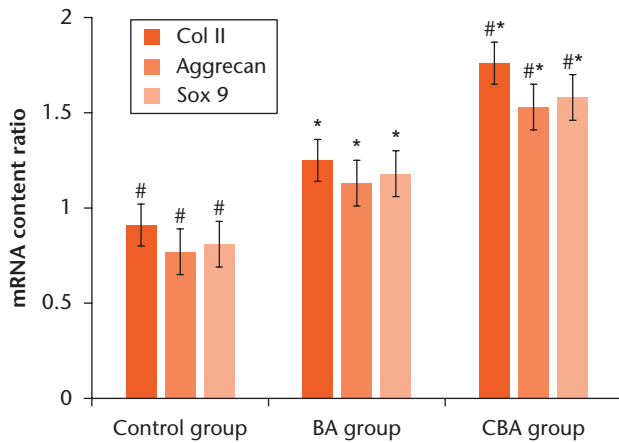


Fig 4

Chart showing the expression of mRNA of collagen II, aggrecan and SOX9 in the samples after they were cultured for one week. Analysis of variance and least-significant differences (LSD) test compared with control group, * $p=0.001$; compared with BA group, # $p=0.001$.

Results

Ratio of chondrocyte detachment. After the chondrocytes were seeded in the scaffold and incubated for four hours, the ratio of detachment was significantly lower in the CBA group than in either the control or BA groups ($p=0.001$ and $p=0.002$, and the ratio of chondrocyte detachment in the control group was 3.82 times higher and 2.11 times higher than the corresponding values in the BA and CBA groups, respectively (Fig. 3).

Real-time PCR. Real-time PCR was used to test the expression of mRNA of collagen II, aggrecan and SOX9 in the samples after they were cultured for one week. As illustrated in Figure 4, all three expressions were highest in the CBA group, followed by the BA group, with the lowest expression in the control group (CBA group > BA group > control group, $p=0.001$ and $p=0.001$).

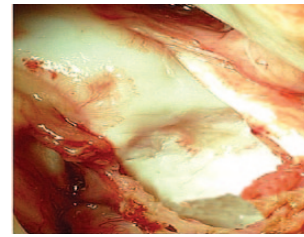


Fig. 5a

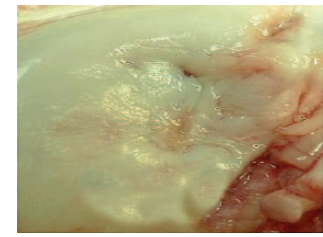


Fig. 5b

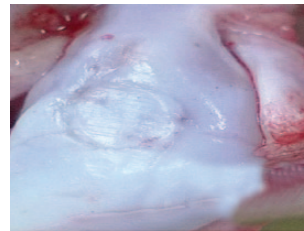


Fig. 5c



Fig. 5d

Macroscopic view of articular cartilage defects in control, BA, CBA, and auto groups at six months post-implantation.

Gross view. The gross appearance of articular cartilage defects in the weight-bearing area was assessed at both 12 and 24 weeks after surgery. The pigs recovered quickly after surgery and at the time of being killed there were no signs of wound infection, limitation of movement or synovitis in the operated knees. No free tissue-engineered cartilage was found away from the cartilage defects in the knee.

All defects in the blank group were mainly occupied by fibrous tissue with little cartilage-like tissue regenerated at 12 weeks post-implantation. The defect was also wider and deeper with the collapse of its adjacent subchondral bone 24 weeks post-implantation. At 12 weeks after implantation, the defects had glossy white, well integrated, regenerated tissue in the CBA and auto groups, although they remained slightly depressed in the centre. Defects in the control group were mostly filled with rough whitish tissue and was clearly distinguishable from the normal cartilage. Defects in the BA group repaired more quickly than those in the control group and slowly than those in the CBA and auto groups. At 24 weeks post-implantation, the defects in the CBA and auto groups were covered by the smooth, consistent, white hyaline tissue almost indistinguishable from the surrounding normal cartilage. No clear signs of margin with normal cartilage could be identified on the surface of the regenerated areas. In contrast, the defects in the control group were partially repaired with fibrous tissue, leaving a small depression in the defect, and the defects in the BA group had a thin irregular surface tissue with obvious defects and cracks surrounding the normal cartilage (Fig. 5).

The grading of all cases according to Moran's criteria in the experimental and control groups is shown in Table I. The auto group had the best repair, indicated by the

Table I. Moran's criteria grading in all groups at different time points

Groups	n	Moran's criteria	
		12 wks after surgery	24 wks after surgery
Control	6	3.35 SD 0.21 ^{††}	3.89 SD 0.22 ^{†‡}
BA	6	3.85 SD 0.21 ^{†‡}	4.45 SD 0.22 ^{†‡}
CBA	6	4.36 SD 0.22 ^{††}	4.98 SD 0.23 ^{††}
Auto	6	4.48 SD 0.23 ^{††}	5.12 SD 0.22 ^{††}

Analysis of variance (ANOVA) and least-significant differences (LSD) test.

Compared with control group

*p = 0.006; compared with BA group

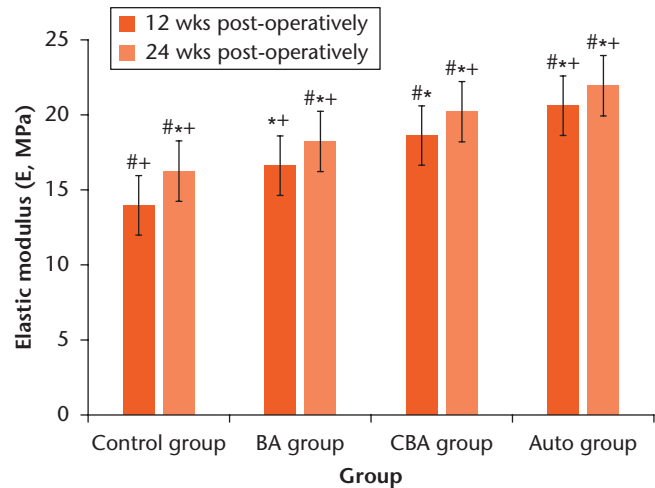
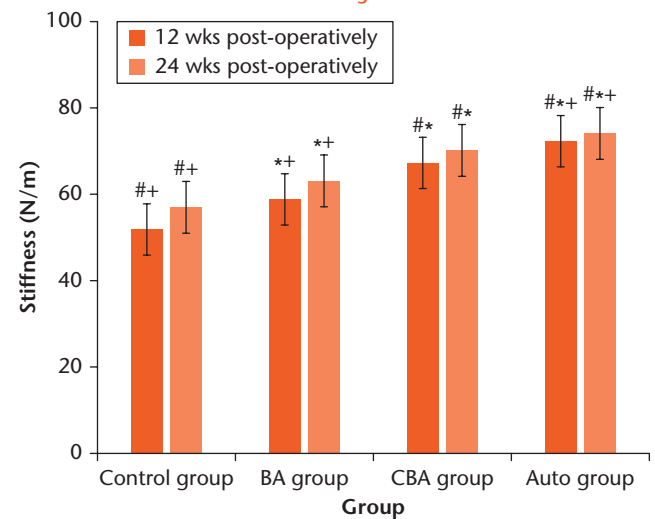
[†]p = 0.009; compared with CBA group

[‡]p = 0.007.

highest grade, both at 12 and 24 weeks after implantation. Although the repair in the CBA group was slightly poorer than in the auto group, there was no statistically significant difference between them ($p = 0.732$). Both the CBA and auto groups were better than the BA group ($p = 0.003$), and the BA group was better than the control group ($p = 0.012$). Meanwhile, the repair improved with time, and was generally better at 24 weeks than at 12 weeks after implantation ($p = 0.004$).

Biomechanical test. The biomechanical properties of the engineered cartilage were determined by measuring the elastic modulus and stiffness. The value was also compared with that of normal cartilage. The biomechanical test was not performed on the samples from the blank group because no cartilage was found. The elastic modulus and stiffness in each group increased with time. At 12 weeks post-implantation, the elastic modulus in the control, BA, CBA and auto groups was 61.2%, 72.8%, 81.6% and 90.3% of the normal cartilage, respectively, and there were significant differences among groups ($p = 0.012$). The stiffness in the control, BA, CBA and auto groups was 68.1%, 77.2%, 88.3% and 94.9% of normal cartilage, respectively ($p = 0.004$). At 24 weeks post-implantation, the elastic modulus in the experimental groups respectively increased to 70.6%, 79.2%, 87.8% and 95.3% of normal cartilage, which had a modulus of 23.02 SD 2.12 MPa. The stiffness in the experimental groups respectively increased to 75.2%, 83.3%, 92.6% and 97.8% of that in normal cartilage, which was 75.76 SD 6.48 N/mm. There were significant differences in the elastic modulus and stiffness between groups ($p < 0.05$). (Fig. 6)

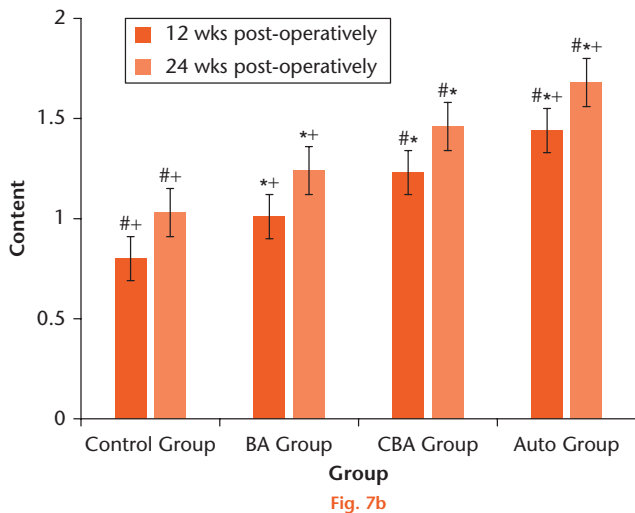
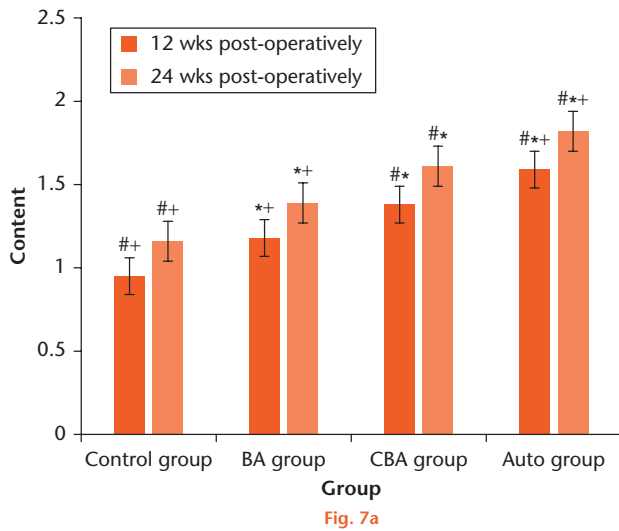
Western blot analyses were performed at 12 and 24 weeks after implantation, and the levels of COL II and aggrecan were determined. The level of expression for each target protein was presented as the ratio of the grey value of the protein band *versus* that of the tubulin band. The results are shown in Figure 7. The COL II and aggrecan in the auto group were the highest at 12 and 24 weeks post-implantation, followed by the CBA group. In contrast, the content in the BA and control groups was much lower. Statistical analysis showed a significant difference between the CBA, BA and control groups ($p < 0.05$) at both 12 and 24 weeks post-implantation.

**Fig. 6a****Fig. 6b**

Biomechanical properties in the four groups at each time point. Analysis of variance (ANOVA) and least-significant differences (LSD) test. Compared with control group, * $p < 0.05$; compared with BA group, # $p < 0.05$; compared with CBA group, + $p < 0.05$ (Western blot analysis).

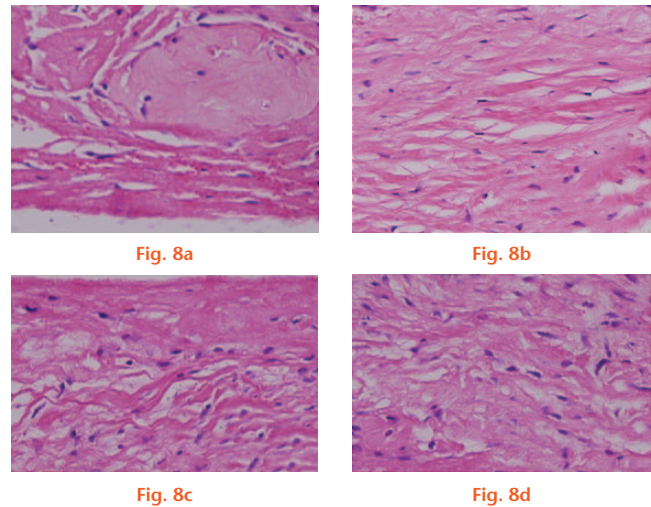
Histological test. The H&E stain at 12 weeks post-implantation showed similar results in the CBA and auto groups. Chondrocytes were arranged in column form with a relatively higher density, and cartilage lacunae were formed. The histological features of the engineered cartilage in these groups were similar to those in normal cartilage. In the control group, the repaired cartilage was distinctly different from that in normal cartilage, with fewer chondrocytes and lacunae. At 24 weeks post-implantation, the defects in the CBA and auto groups were repaired by newly generated hyaline cartilage (Fig. 8).

Deposition of GAG in the engineered cartilage was confirmed by TB staining at 12 and 24 weeks post-implantation. The staining showed superiority of the 24-week engineered cartilage construct over the 12-week samples in terms of cartilage-specific ECM. At 12 weeks post-implantation, the defects in the CBA and auto

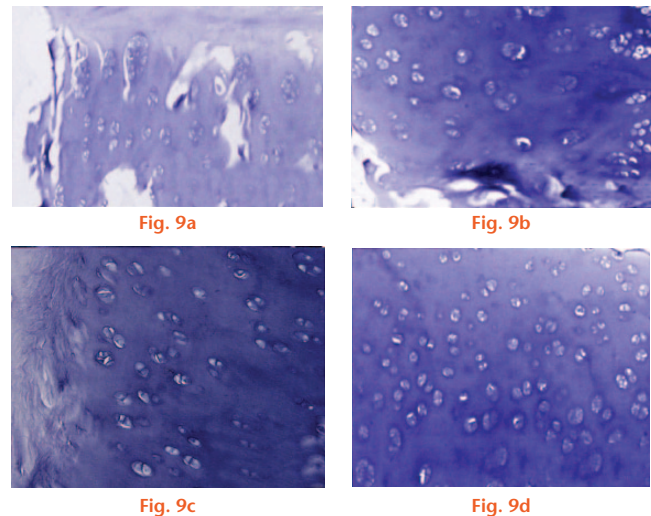


Charts showing comparison of the a) aggrecan and b) COL II content in the control, BA, CBA and Auto group after surgery. Analysis of variance (ANOVA) and least-significant differences (LSD) test. Compared with control group, * $p < 0.05$; compared with BA group, # $p < 0.05$; compared with CBA group, + $p < 0.05$.

groups were filled with regenerated cartilage similar to a mixture of hyaline cartilage and abundant ECM, as shown by TB staining. However, the arrangement of the cells in the new cartilage still lacked zonal organisation. The TB staining in the BA group was better than in the control group but worse in the range and density than in the CBA group. At 24 weeks, the repaired sites in the CBA and auto groups showed uniform, positive staining for cartilaginous ECM, comparable with that of normal cartilage. The 24-week TB staining showed that the engineered cartilage in the CBA group was better than that in the BA group, while the engineered cartilage was poorest in the control group (Fig. 9). The positively dyed region and the degree of staining in the control group clearly distinguished the engineered tissue from normal tissue, with some asymmetrical and blurred distribution



At 24 weeks post-implantation, the defects in the c) CBA and d) auto groups were repaired by newly generated hyaline cartilage shown by the formation of lacunae and cell clusters. The new-formed cartilage integrated well with its adjacent cartilage, although the interface between engineered and normal cartilage could still be identified. However, there were few cells and lacunae in the control group a). The BA group b) showed better results in terms of healing ability compared with the control group, but worse than those in the CBA group, haematoxylin and eosin $\times 200$.



At 24 weeks, the repaired sites in the c) CBA and d) auto groups displayed uniform, positive staining for cartilaginous ECM, comparable with that of normal cartilage. The results of the 24-week TB staining showed that the engineered cartilage in the CBA group c) was better than that in the BA group b), while the engineered cartilage in the control group a) was the poorest among the groups, TB $\times 200$.

of matrix. Part of the region still lacked matrix and stained lightly.

Histological scoring results. The repair was evaluated using the scoring system of Wakitani et al,³¹ in which the total is 14, and a lower score signifies a better effect. The auto group had the best effect at both 12 and 24 weeks post-implantation (Table II), although the scores in the CBA group were slightly poorer than those in the

Table II. Results of Wakitani histological scoring

Groups	n	Wakitani histological scoring	
		12 wks after surgery	24 wks after surgery
Control	6	7.08 SD 0.33 ^{††}	6.12 SD 0.31 ^{††}
BA	6	6.26 SD 0.32 ^{*‡}	5.37 SD 0.33 ^{*‡}
CBA	6	5.12 SD 0.29 ^{††}	4.41 SD 0.32 ^{††}
Auto	6	4.97 SD 0.31 ^{††}	4.26 SD 0.29 ^{††}

Analysis of variance (ANOVA) and least-significant differences (LSD) test.

Compared with control group

* $p = 0.003$; compared with BA group

† $p = 0.007$; compared with CBA group

‡ $p = 0.006$.

auto group, and there were no significant differences ($p > 0.05$). The scores in the CBA and auto groups were better than in the BA group ($p < 0.05$) whose scores were better than in the control group ($p < 0.05$). Furthermore, the engineered cartilage scores in each group at 24 weeks post-implantation were significantly better than their corresponding scores at 12 weeks ($p = 0.003$).

Results of the immunohistochemical staining. Immunohistochemical staining was consistent with the TB staining, and showed better quality and quantity of repair in the CBA group compared with the BA group and the controls. At 12 weeks post-implantation, an even distribution and expanded darker positive immunohistochemical staining of COL II was seen in the CBA and auto groups, indicating the presence of hyaline cartilage in the regenerated tissue. In contrast, the staining of the control group and the BA group showed an abundance of collagen II in the regenerated tissue, indicating the minimal production, or complete absence, of hyaline cartilage. At 24 weeks post-implantation, with the maturation of engineered cartilage, the expression and distribution of COL II in the CBA and auto groups were similar to those of normal cartilage, with positive staining of the ECM around the evenly distributed chondrocyte-like cells at the site of the repair. Most of the scaffolds in the CBA group were degraded, endocytosed, and replaced. The BA group had better results than the control group but worse results than the CBA group (Fig. 10).

Discussion

Functionally, cartilage in the weight-bearing area is the major structure in the knee joint to be responsible for the compression, transmission and absorption of forces. It has been shown that more than 80% of patients suffering full-thickness defects in weight-bearing areas may develop OA within five to ten years.³² The restoration of defects in weight-bearing areas is thus more important than that in non-weight-bearing areas.³³ However, most of the data regarding tissue-engineered cartilage come from results in small animal models. Although commonly used and significantly less expensive, small animal models such as rabbits and rodents do not give useful information. For instance, cartilage defects in rabbits tend to

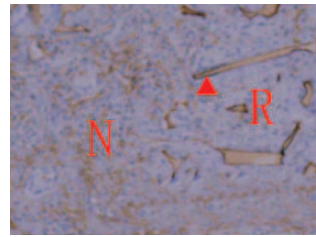


Fig. 10a

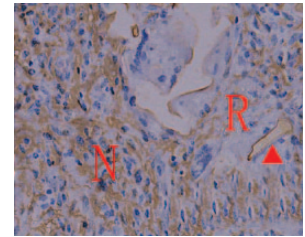


Fig. 10b

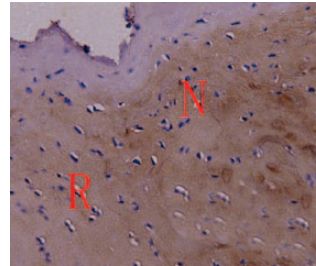


Fig. 10c

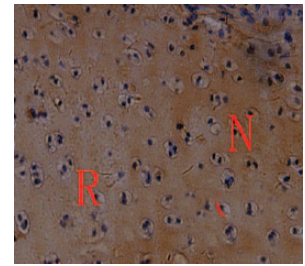


Fig. 10d

At 24 weeks after surgery, with the maturation of engineered cartilage, the expression and distribution of COL II in the c) CBA and d) auto groups were similar to those of normal cartilage, with positive staining of the ECM matrix around the evenly distributed chondrocyte-like cells at the site of the repair tissue. Most of the scaffolds in the CBA group were degraded, endocytosed, and replaced. The BA group b) had better results than the control group a) but worse results than the CBA group. ▲: traces of the scaffold; R, regenerated tissue; N: normal tissue.

heal spontaneously, and it is difficult to create purely chondral defects in rodents due to the extremely thin layer of cartilage.³⁴ The use of large animal models may be more appropriate for the translation of methods of treating cartilage defects in humans. For example, the size and the gait characteristics of the porcine knee more accurately reflect those in humans than do those of smaller animals.³⁴ It is a primary focus of orthopaedic research to develop reliable models for the investigation of the repair or regeneration of damaged articular cartilage. Tissue engineering and regenerative medicine have shown great promise in this regard by using a 3D scaffold seeded with cells,³⁵ and the success of tissue-engineered repair of cartilage may depend on the rapid and efficient adhesion of transplanted cells to the scaffold.

Accordingly, in the present study, a full-thickness articular cartilage defect was created in a weight-bearing porcine model, and the CD44 monoclonal antibody biotin-avidin (CBA) binding technique was used to construct the tissue-engineered cartilage. The defects were repaired with tissue-engineered cartilage constructed with the CBA binding technique three and six months post-operatively.

Previously, the BA technique was used to enhance the adhesion of chondrocytes, however, endocytosis of biotin molecules by chondrocytes decreased the strength of adhesion between the biotinylated cells and avidin-coated substrata, undermining the use of this system.²⁸ It has been reported that endocytosis can be weakened greatly when the temperature of the culture drops to

4°C. However, this temperature can reduce the survival and the ability of the cells to proliferate.²⁴

In our previous study, the combination of the BA system and monoclonal anti-CD44 antibodies was applied in order to enhance the adhesion of chondrocytes and the regeneration of cartilage in porous scaffolds, and we found that the CBA technique can enhance the adhesion between chondrocytes and 3D chitosan scaffold *in vitro*.²⁷ In the current study, we found that the rate of detachment was greatly reduced by the CBA technique at four hours after implantation. Real-time PCR results at one week after implantation showed an increase in the levels of expression of COL II, aggrecan and SOX9 in the CBA group. These results further show that the CBA technique can improve the adhesion between chondrocytes and the scaffold, promoting the proliferation of cells and ensuring expression of the phenotype. This is consistent with our previous *in vitro* studies.²⁷

The pigs in this study recovered well post-implantation without local complications. The surgical process is simple and safe. The chondral defect with a diameter of 10 mm and depth of 3 mm cannot spontaneously repair in a porcine model, and thus is of critical size.^{36,37} Indeed, none of the animals in the blank group had full cartilaginous repair 12 or 24 weeks post-implantation.

The biomechanical results revealed that the Elastic modulus and stiffness in the auto group were significantly greater than those in the CBA group. The Elastic modulus and stiffness in the CBA group were significantly greater than those in the BA and control group. It is clear that although the same biomechanical properties could not be reached using the CBA technique as when using the autologous transplant technique, it is much better than both the BA technique and the control group. The better biomechanical properties could guarantee restoration of the load-bearing function and performance of the repaired cartilage, and it can potentially restore the function of the cartilage, which was further proved by the results of the histological and Western blot test.

As shown histologically, the defect repaired with engineered cartilage constructed using CBA techniques at six months post-implantation has an architecture that is characteristic of mature hyaline cartilage. Mature chondrocytes distributed evenly in the ECM were found in both the CBA and autologous groups. They were less mature and with a more uneven distribution in the BA and control groups. As the most important components of ECM in hyaline cartilage, the level of COL II and aggrecan were found to be expressed in the engineered tissue at three months post-implantation and this was enhanced at six months post-implantation in each group. Results of the Western blot analysis revealed that COL II and aggrecan were highest in the autologous group, followed by the CBA group, and then the BA group and the control group.

The TB staining also showed the deposition of GAG in the engineered cartilage. This is another major component responsible for maintaining the water content and biomechanical properties of hyaline cartilage. The biochemical composition (GAG quantification) and biomechanical properties (compressive modulus) of engineered cartilage six months post-implantation were similar to those of normal cartilage, indicating that the defects were repaired both structurally and functionally.

Taken together, these results suggest that regeneration of a specific hyaline cartilage to repair cartilage defects in weight-bearing areas could be achieved using tissue-engineered cartilage constructed with the CBA technique. Although the same repair could not be achieved in the CBA group as in autologous group, the results in these two groups were similar when assessed using Moran's criteria and Wakitani histological scoring.

In conclusion, it is clear that the CBA technique used in this study is an effective means of improving the adhesion between chondrocytes and scaffolds. Tissue-engineered cartilage constructed using the CBA technique was found to repair cartilage defects in weight-bearing areas in pigs effectively, although the repair remains imperfect. Tissue-engineered cartilage constructed using this technique may therefore potentially be used to repair cartilage defects in weight-bearing areas of joints.

Supplementary material

 Tables showing grading according to Moran's criteria and the results of Wakitani histological scoring. can be found alongside this paper at <http://www.bjr.boneandjoint.org.uk/>

References

1. Heir S, Nerhus TK, Røtterud JH, et al. Focal cartilage defects in the knee impair quality of life as much as severe osteoarthritis: a comparison of knee injury and osteoarthritis outcome score in 4 patient categories scheduled for knee surgery. *Am J Sports Med* 2010;38:231-237.
2. Hootman JM, Helmick CG, Brady TJ. A public health approach to addressing arthritis in older adults: the most common cause of disability. *Am J Public Health* 2012;102:426-433.
3. Mobasheri A, Csaki C, Clutterbuck AL, Rahmizadeh M, Shakibaei M. Mesenchymal stem cells in connective tissue engineering and regenerative medicine: applications in cartilage repair and osteoarthritis therapy. *Histol Histopathol* 2009;24:347-366.
4. Ahmed TA, Hincke MT. Strategies for articular cartilage lesion repair and functional restoration. *Tissue Eng Part B Rev* 2010;16:305-329.
5. Mollon B, Kandel R, Chahal J, Theodoropoulos J. The clinical status of cartilage tissue regeneration in humans. *Osteoarthritis Cartilage* 2013;21:1824-1833.
6. Brittberg M. Cell carriers as the next generation of cell therapy for cartilage repair: a review of the matrix-induced autologous chondrocyte implantation procedure. *Am J Sports Med* 2010;38:1259-1271.
7. Goyal D, Keyhani S, Lee EH, Hui JH. Evidence-based status of microfracture technique: a systematic review of level I and II studies. *Arthroscopy* 2013;29:1579-1588.
8. Mithoefer K. Complex articular cartilage restoration. *Sports Med Arthrosc* 2013;21:31-37.
9. Schindler OS. Cartilage repair using autologous chondrocyte implantation techniques. *J Perioper Pract* 2009;19:60-64.
10. Cui L, Wu Y, Cen L, et al. Repair of articular cartilage defect in non-weight bearing areas using adipose derived stem cells loaded polyglycolic acid mesh. *Biomaterials* 2009;30:2683-2693.

11. **Makris EA, Gomoll AH, Malizos KN, Hu JC, Athanasiou KA.** Repair and tissue engineering techniques for articular cartilage. *Nat Rev Rheumatol* 2015;11:21-34.
12. **Wang W, Li B, Yang J, et al.** The restoration of full-thickness cartilage defects with BMSCs and TGF-beta 1 loaded PLGA/fibrin gel constructs. *Biomaterials* 2010;31:8964-8973.
13. **Anderson JA, Little D, Toth AP, et al.** Stem cell therapies for knee cartilage repair: the current status of preclinical and clinical studies. *Am J Sports Med* 2014;42:2253-2261.
14. **Mahmood TA, de Jong R, Riesle J, Langer R, van Blitterswijk CA.** Adhesion-mediated signal transduction in human articular chondrocytes: the influence of biomaterial chemistry and tenascin-C. *Exp Cell Res* 2004;301:179-188.
15. **Liu X, Wang S.** Three-dimensional nano-biointerface as a new platform for guiding cell fate. *Chem Soc Rev* 2014;43:2385-2401.
16. **Wang X, Gan H, Zhang M, Sun T.** Modulating cell behaviors on chiral polymer brush films with different hydrophobic side groups. *Langmuir* 2012;28:2791-2798.
17. **Berns EJ, Sur S, Pan L, et al.** Aligned neurite outgrowth and directed cell migration in self-assembled monodomain gels. *Biomaterials* 2014;35:185-195.
18. **Wu EC, Zhang SG, Hauser CAE.** Self-Assembling Peptides as Cell-Interactive Scaffolds. *Adv Funct Mater* 2012;22:456-468.
19. **Zhang Z, Lai Y, Yu L, Ding J.** Effects of immobilizing sites of RGD peptides in amphiphilic block copolymers on efficacy of cell adhesion. *Biomaterials* 2010;31:7873-7882.
20. **Green NM.** Avidin. 3. The nature of the biotin-binding site. *Biochem J* 1963;89:599-609.
21. **Green NM.** Avidin. *Adv Protein Chem* 1975;29:85-133.
22. **Wang B, Song J, Yuan H, et al.** Multicellular assembly and light-regulation of cell-cell communication by conjugated polymer materials. *Adv Mater* 2014;26:2371-2375.
23. **Gong PY, Zheng WF, Huang Z, et al.** A Strategy for the Construction of Controlled, Three-Dimensional, Multilayered, Tissue-Like Structures. *Adv Funct Mater* 2013;23:42-46.
24. **Tsai WB, Wang PY, Chang Y, Wang MC.** Fibronectin and culture temperature modulate the efficacy of an avidin-biotin binding system for chondrocyte adhesion and growth on biodegradable polymers. *Biotechnol Bioeng* 2007;98:498-507.
25. **Grover J, Roughley PJ.** Expression of cell-surface proteoglycan mRNA by human articular chondrocytes. *Biochem J* 1995;309:963-968.
26. **Salter DM, Godolphin JL, Gourlay MS, et al.** Analysis of human articular chondrocyte CD44 isoform expression and function in health and disease. *J Pathol* 1996;179:396-402.
27. **Lin H, Zhou J, Shen L, et al.** Biotin-conjugated anti-CD44 antibody-avidin binding system for the improvement of chondrocyte adhesion to scaffolds. *J Biomed Mater Res A* 2014;102:1140-1148.
28. **Tsai WB, Wang MC.** Effect of an avidin-biotin binding system on chondrocyte adhesion, growth and gene expression. *Biomaterials* 2005;26:3141-3151.
29. **Moran ME, Kim HK, Salter RB.** Biological resurfacing of full-thickness defects in patellar articular cartilage of the rabbit. Investigation of autogenous periosteal grafts subjected to continuous passive motion. *J Bone Joint Surg [Br]* 1992;74-B:659-667.
30. **Zhou G, Liu W, Cui L, et al.** Repair of porcine articular osteochondral defects in non-weightbearing areas with autologous bone marrow stromal cells. *Tissue Eng* 2006;12:3209-3221.
31. **Wakitani S, Goto T, Pineda SJ, et al.** Mesenchymal cell-based repair of large, full-thickness defects of articular cartilage. *J Bone Joint Surg [Am]* 1994;76-A:579-592.
32. **Hangody L, Módis L.** [Surgical treatment options for weight bearing articular surface defect]. *Orv Hetil* 2006;147:2203-2212. [Article in Hungarian]
33. **Dragoo JL, Carlson G, McCormick F, et al.** Healing full-thickness cartilage defects using adipose-derived stem cells. *Tissue Eng* 2007;13:1615-1621.
34. **Cook JL, Hung CT, Kuroki K, et al.** Animal models of cartilage repair. *Bone Joint Res* 2014;3:89-94.
35. **Ochi M, Adachi N, Nobuto H, et al.** Articular cartilage repair using tissue engineering technique—novel approach with minimally invasive procedure. *Artif Organs* 2004;28:28-32.
36. **Gotterbarm T, Breusch SJ, Schneider U, Jung M.** The minipig model for experimental chondral and osteochondral defect repair in tissue engineering: retrospective analysis of 180 defects. *Lab Anim* 2008;42:71-82.
37. **Chu CR, Szczodry M, Bruno S.** Animal models for cartilage regeneration and repair. *Tissue Eng Part B Rev* 2010;16:105-115.

Funding Statement

- National Natural Science Foundation of China (Grant number: 81301577, 30872623); Shanghai Rising-Star Program (Grant number 15QA1401000); Foundation for Medical Guide Program of Shanghai Science and Technology (Grant number: 16401933000).
- H. Lin and J. Zhou contributed equally to this paper.

Author Contribution

- H. Lin: Carried out experiments, analysed experimental results, wrote the paper
- J. Zhou: Carried out experiments, wrote paper.
- L. Cao: Assisted with performing animal experiments.
- H. R. Wang: Assisted with analysing results.
- J. Dong: Designed experiments.
- Z. R. Chen: Designed experiments.

ICMJE COI Statement

- None declared.

© 2017 Chen et al. This is an open-access article distributed under the terms of the Creative Commons Attribution licence (CC-BY-NC), which permits unrestricted use, distribution, and reproduction in any medium, but not for commercial gain, provided the original author and source are credited. Usapit laboreni cumquatrem labore volu